Calculation of spectral line profiles of multielectron emitters in plasmas

L. A. Woltz
Atomic and Plasma Radiation Division, Center for Radiation Research, National Bureau of Standards, Gaithersburg, Maryland 20899

C. F. Hooper, Jr.
Department of Physics, University of Florida, Gainesville, Florida 32611
(Received 17 March 1988)

A theoretical formalism and computer code have been developed to calculate spectra of multielectron emitters in plasmas. The plasma electron broadening is treated by a quantum-mechanical relaxation theory. The static-ion approximation is used to treat plasma ion broadening of the atomic levels. Calculated lithiumlike and berylliumlike krypton spectra are compared to experimental spectra obtained in laser implosion experiments at the Laboratory for Laser Energetics, University of Rochester.

I. INTRODUCTION

In this paper we describe a formalism and computer code which have been developed to calculate theoretical spectral line profiles for a general multielectron emitter in a plasma, using data for atomic energy levels and radial matrix elements calculated by atomic structure programs. These line profile calculations are presently done using the static-ion approximation, in which the plasma ions which perturb the emitting ion, or radiator, are assumed to have negligible motion during the average lifetime of the radiator excited states. The microfield due to the plasma ions can cause shifts and splittings of the energy levels of the radiator; and it can mix radiator states of opposite parity, permitting transitions which are not allowed in the absence of the field. A quantum-mechanical relaxation theory is used to calculate the plasma electron broadening of the spectral lines.[1] The form of this line profile calculation could also permit an impact[2] or unified theory[3] treatment of electron broadening to be employed. It should also be possible to include the effects of ion dynamics within this formulation.[4]

We use this program to calculate the $N=3$ to 2 and $N=4$ to 2 lithiumlike and berylliumlike krypton spectra in plasmas having electron densities of 10^{23} to 10^{24} cm^{-3} and a temperature of 1100 eV, and compare our theoretical spectra to experimental spectra obtained in laser-produced plasma experiments at the Laboratory for Laser Energetics, University of Rochester (LLE).

II. LINE PROFILES IN THE STATIC-ION APPROXIMATION

The spectral line profile, in the static-ion approximation, is given by[2]

$$I(\omega)=\int_0^\infty P(\epsilon)J(\omega,\epsilon)d\epsilon\ , \tag{1}$$

where $P(\epsilon)$ is the static-ion microfield probability distribution[5] and $J(\omega,\epsilon)$ gives the electron-broadened profile for a given ion field strength ϵ:

$$J(\omega,\epsilon)=-\frac{1}{\pi}\mathrm{Im}\sum_{ifi'f'}\rho_i\mathbf{d}_{f'i'}\cdot[\omega-L_R(\epsilon)-M(\omega)]^{-1}_{i'f',if}\mathbf{d}_{if}\ . \tag{2}$$

Here, i,f represent initial and final radiator states, $L_R(\epsilon)$ is the radiator Liouville operator, which is a commutator of the radiator Hamiltonian:

$$L_R(\epsilon)\equiv[H_R(\epsilon),]\ ,$$

$\mathbf{d}$ is the radiator dipole operator, ρ is the radiator density operator, and $M(\omega)$ is the electron broadening operator.

The sum in Eq. (2) can be considered as the trace of the product of two matrices, $\mathbf{d}\cdot\mathbf{d}$ and $[\omega-L_R(\epsilon)-M(\omega)]^{-1}$, where the rows and columns of the matrices are indexed by the pairs (i,f). If a field-dependent atomic basis set were used to calculate the line profile, forbidden transitions would appear explicitly for nonzero field as diagonal matrix elements of the dipole transition matrix, $\mathbf{d}\cdot\mathbf{d}$. Since the trace of a matrix is invariant under unitary transformations, the same result can be obtained using a field-independent basis set, which is what we have done in this calculation.

For the work presented here, $M(\omega)$ was calculated to second order in the radiator-electron interaction for which the dipole approximation was used. Higher multipoles might be significant in the electron broadening,[6,7] but they were not considered. The electron widths obtained here were less than those due to Doppler and source broadening for electron densities less than 10^{24} cm^{-3}, so the dipole approximation should not cause significant errors in our experimental analysis. Using these approximations, elements of the tetradic electron broadening operator can be written in the form[8]

$$M(\omega)_{if,i'f'}=-\frac{2ie^4n_e}{3\hbar^2}\left[\frac{8\pi m}{kT}\right]^{1/2}\left\{\delta_{ff'}\sum_{i''}\mathbf{R}_{ii''}\cdot\mathbf{R}_{i''i'}G(\Delta\omega_{i''f})+\delta_{ii'}\sum_{f''}\mathbf{R}_{f'f''}\cdot\mathbf{R}_{f''f}G(-\Delta\omega_{if''})-\mathbf{R}_{ii'}\cdot\mathbf{R}_{f'f}[G(\Delta\omega_{if'})+G(-\Delta\omega_{i'f})]\right\}, \tag{3}$$

where n_e is the plasma electron density, m is the electron mass, $\mathbf{R}$ is the radiator electron position operator, and $G(\omega)$ is a function which represents the effects of the perturbing electrons. The calculation of $G(\omega)$ involves a trace over perturbing electron wave functions, which were taken to be Coulomb wave functions.[1] To obtain this form for $M(\omega)$, the no-quenching approximation has been made; i.e., all matrix elements of $\mathbf{R}$ between initial and final radiator states are set equal to zero. When this approximation is not made, $M(\omega)$ takes on a more complicated form.

III. MULTIELECTRON RADIATORS

In order to calculate a spectral line profile for a multielectron radiator using Eqs. (1)–(3), matrix elements of the atomic operators $\mathbf{d}$, $\mathbf{R}$, and z are needed. Matrix elements of $\mathbf{d}$ (and similarly for $\mathbf{R}$) are given by

$$\langle\gamma_iJ_iM_i\,|\,d_q\,|\,\gamma_fJ_fM_f\rangle=e(-1)^{J_i-M_i}\begin{pmatrix}J_i & 1 & J_f\\ -M_i & q & M_f\end{pmatrix}\langle\gamma_iJ_i\|P^{(1)}\|\gamma_fJ_f\rangle\,, \tag{4}$$

where $\langle\gamma_iJ_i\|P^{(1)}\|\gamma_fJ_f\rangle$ is a reduced radial matrix element of the radiator electron position operator, $P_q^{(1)}=\sum_{i=1}^{N}r_q^{(1)}(i)$; and d_q is a spherical tensor component of $\mathbf{d}$. The ket $|\,\gamma_iJ_iM_i\rangle$ represents a state of the radiator: J_i and M_i are angular momentum quantum numbers and γ_i represents all other quantum numbers of the state. The notation used here is from Cowan's text on atomic physics.[9]

Using Eq. (4), the term $\mathbf{d}_{if'}\cdot\mathbf{d}_{f'i'}$, which appears in Eq. (2), can be written

$$\mathbf{d}_{if'}\cdot\mathbf{d}_{f'i'}=e^2(-1)^{J_i+J_{f'}-M_{f'}-M_f}\begin{pmatrix}J_i & 1 & J_f\\ -M_i & M_i-M_f & M_f\end{pmatrix}\begin{pmatrix}J_{f'} & 1 & J_{i'}\\ -M_{f'} & M_f-M_i & M_{i'}\end{pmatrix}\times\langle\gamma_iJ_i\|P^{(1)}\|\gamma_fJ_f\rangle\langle\gamma_{f'}J_{f'}\|P^{(1)}\|\gamma_{i'}J_{i'}\rangle\delta_{M_i-M_f,M_{i'}-M_{f'}}\,. \tag{5}$$

The term

$$\sum_{i''}\mathbf{R}_{ii''}\cdot\mathbf{R}_{i''i'}G(\Delta\omega_{i''f})\,,$$

which appears in Eq. (3) for $M(\omega)$, can be written as

$$\sum_{i''}\mathbf{R}_{ii''}\cdot\mathbf{R}_{i''i'}G(\Delta\omega_{i''f})=\sum_{\gamma_{i''}J_{i''}}(-1)^{J_i-J_{i''}}(2J_i+1)^{-1}\delta_{J_iJ_{i'}}\delta_{M_iM_{i'}}\langle\gamma_iJ_i\|P^{(1)}\|\gamma_{i''}J_{i''}\rangle\langle\gamma_{i''}J_{i''}\|P^{(1)}\|\gamma_{i'}J_{i'}\rangle G(\Delta\omega_{\gamma_{i''}J_{i''},\gamma_fJ_f})\,. \tag{6}$$

The radiator Hamiltonian in the presence of an ion field is given by

$$H_R(\epsilon)=H_R(0)+e\epsilon\cdot\mathbf{R} \tag{7}$$

or by

$$H_R(\epsilon)=H_R(0)+e\epsilon z \tag{8}$$

if the z axis is chosen to be in the direction of ϵ. The matrix element of z is

$$\langle\gamma_iJ_iM_i\,|\,z\,|\,\gamma_{i'}J_{i'}M_{i'}\rangle=(-1)^{J_i-M_i}\begin{pmatrix}J_i & 1 & J_{i'}\\ -M_i & 0 & M_i\end{pmatrix}\delta_{M_iM_{i'}}\times\langle\gamma_iJ_i\|P^{(1)}\|\gamma_{i'}J_{i'}\rangle\,. \tag{9}$$

With this formulation of the line broadening problem, the atomic data that are needed as input are the radiator energy levels—matrix elements of $H_R(0)$ in Eq. (8), and the reduced radial matrix elements,

$$\langle\gamma_iJ_i\|P^{(1)}\|\gamma_{i'}J_{i'}\rangle\,,$$

$$\langle\gamma_iJ_i\|P^{(1)}\|\gamma_fJ_f\rangle\,,$$

and

$$\langle\gamma_fJ_f\|P^{(1)}\|\gamma_{f'}J_{f'}\rangle\,,$$

which appear in Eqs. (5), (6), and (9).

IV. SELECTION OF ATOMIC STATES FOR THE LINE PROFILE CALCULATION

In general, the indices i, f, i', f' of Eqs. (2) and (3) would each range over all states of the radiator. In a practical application, only a small subset of the matrix

elements of **d** and **R** contribute significantly to the line emission in a given range of energies. The significant elements of **d** are those which correspond to transition energies which lie within or near the spectral energy range to be studied. All other elements of **d** can be neglected. This usually restricts the sets of initial states and final states to two nonoverlapping energy ranges. Again, usually these ranges are separated sufficiently so that the matrix elements of **R** of the form $\mathbf{R}_{if}$ are negligible in comparison with those of the form $\mathbf{R}_{ii'}$. The no-quenching approximation is the neglect of the elements $\mathbf{R}_{if}$ in the calculation of $M(\omega)$. In Eq. (3) a term of the form $\mathbf{R}_{ii''}\cdot\mathbf{R}_{i''i'}$ or $\mathbf{R}_{ff''}\cdot\mathbf{R}_{f''f'}$ appears. The states i'',f'' are called perturbing states. All perturbing states which contribute significantly to the electron broadening must be included. Usually, this only includes states i'' (f'') within or near the energy range of the set of initial (final) states.

In calculations presented in this paper the no-quenching approximation is used; and it is assumed that the energy range of the set of initial states plus initial perturbing states does not overlap the energy range of the set of final states plus final perturbing states. The formalism can easily be extended to include quenching, but the size of the calculated matrices will increase greatly.

V. MATRIX CALCULATIONS

The tetradic operator $[\omega-L_R(\epsilon)-M(\omega)]$, which appears in Eq. (2), must be calculated and inverted to obtain the spectrum. The neglect of matrix elements of the form $\mathbf{d}_{ii'}$, $\mathbf{d}_{ff'}$, and $\mathbf{R}_{if}$ greatly simplifies the calculation of $[\omega-L_R(\epsilon)-M(\omega)]$; only elements of the form $[\omega-L_R(\epsilon)-M(\omega)]_{if,i'f'}$ are required. The operator can be put into the form of a matrix if each pair of subscripts i,f is represented by a single integer j which indexes the rows and columns of $[\omega-L_R(\epsilon)-M(\omega)]$. The inversion can then be done by numerical matrix inversion.

The matrix $[\omega-L_R(\epsilon)-M(\omega)]$ can be quite large, but it does have, at least in certain approximations, a block-diagonal form. The computer program which calculates the spectrum determines the block diagonalization and does the calculation using the matrix blocks.

Further approximations which are optional in the program but which may be necessary due to limits of computer size or time are the neglect of lower state broadening [the second term of Eq. (3)], the neglect of interference terms [the last term of Eq. (3)], and the neglect of ion field induced shifts of the lower states [matrix elements $\langle f \mid z \mid f' \rangle$ in Eq. (8)]. These approximations are good if, as is often the case, the final states of the transitions of interest are much less affected by plasma perturbations than are the initial states.

VI. COMPARISON WITH SPECTRA FROM LASER-PRODUCED PLASMAS

Laser implosion experiments have been done recently at LLE using targets which contained a mixture of argon and krypton gases. Details of these experiments are discussed by Delamater *et al.*[10] The x-ray spectra obtained in these experiments contain spectral lines from hydrogenic and heliumlike argon, and also lines from lithiumlike and berylliumlike krypton. Here we show theoretical spectra for the $N=3$ to 2 and $N=4$ to 2 transitions of Li-like and Be-like Kr, and compare them with the LLE time-integrated spectra. We examine the density dependence of these spectra in order to determine their sensitivity and hence their usefulness as a density diagnostic for laser implosion experiments.

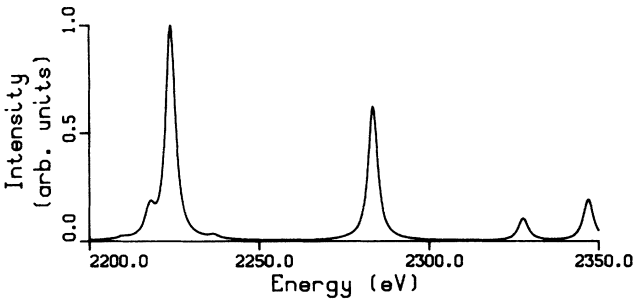

FIG. 1. Lithiumlike krypton spectrum, 2200–2350 eV, $N=3$ to 2 transitions. Electron density, 1.5×10^{23} cm^{-3}; temperature, 1100 eV.

The atomic data used in generating these spectra were calculated with the atomic structure codes of Cowan.[9] The microfield probability distributions were calculated with the codes of Tighe and Hooper.[5] The approximations of no lower state broadening, no interference terms, and no ion field induced lower state shifts were used in calculating the spectra presented here. Sample calculations were done for the Li-like Kr $N=4$ to 2 spectra including lower state broadening and lower state shift; and they were found to be in close agreement with the spectra in which these effects were omitted. The radiator density operator ρ was taken to be the Boltzmann factor in this work; but it could be changed to represent non-LTE plasma conditions.

In Figures 1 and 2 we show theoretical Li-like and Be-like Kr spectra for $N=3$ to 2 transitions in the energy range 2200–2350 eV. These are calculated for an elec-

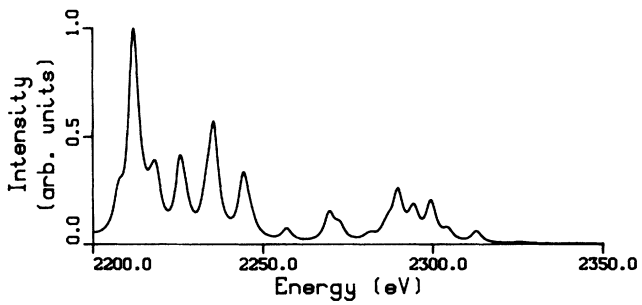

FIG. 2. Berylliumlike krypton spectrum, 2200–2350 eV, $N=3$ to 2 transitions. Electron density, 1.5×10^{23} cm^{-3}; temperature, 1100 eV.

tron density of 1.5×10^{23} cm^{-3} and a temperature of 1100 eV. In all theoretical spectra in this paper, the Stark-broadened profiles have been convoluted with a Doppler profile and with a 1.5-eV half-width at half maximum (HWHM) Lorentzian to simulate the source broadening which is present in the experimental spectra. Figure 3 shows a comparison of the combined spectra of Figs. 1 and 2 to the LLE x-ray spectrum from shot 11582 for the energy range 2200–2350 eV. The experimental spectrum in this energy range is composed predominately of lines from Li-like and Be-like Kr $N=3$ to 2 transitions. The plasma conditions used for these theoretical spectra were indicated by analysis of the hydrogenic and He-like Ar spectral lines from shot 11582.[10] The linewidths obtained in this figure are due predominately to Doppler and source broadening. Even at electron densities of 10^{24} cm^{-3} there is little change in the calculated spectra; so for densities $<10^{24}$ cm^{-3}, the Stark broadening of the $N=3$ to 2 Li-like and Be-like Kr lines is too small for these lines to be of use as a density diagnostic.

The Li-like Kr spectral lines from $N=4$ to 2 transitions do, however, show significant Stark broadening at 10^{23} cm^{-3}; and the $N=4$ to 2 Be-like Kr lines show significant Stark broadening at 10^{24} cm^{-3}. Figure 4 shows theoretical Li-like Kr spectra for the energy range 2900–3100 eV, a temperature of 1100 eV, and densities of 10^{23}, 2×10^{23}, 4×10^{23}, and 10^{24} cm^{-3}. Over this density range there is a large change in the linewidths and shapes; at the upper end of the density range the ion microfield splits each of the two main peaks into two components. This broadening and splitting of the Li-like peaks should be a fairly sensitive density diagnostic for densities $>10^{23}$ cm^{-3}. Figure 5 shows theoretical Be-like Kr spectra for electron densities of 1.5×10^{23} and 10^{24} cm^{-3}, and a temperature of 1100 eV. At 1.5×10^{23} cm^{-3}, the broadening is mainly Doppler and source broadening, but at 10^{24} cm^{-3}, Stark broadening is the predominant broadening mechanism. At 10^{24} cm^{-3}, the ion microfield has significantly changed relative peak intensities from those at 1.5×10^{23} cm^{-3}. At this highest density, errors due to the neglect of electron degeneracy will be on the order of 1%.[11] Figure 6 shows combined spectra for Li-like and Be-like Kr at densities of 2×10^{23} and 10^{24} cm^{-3}, and a temperature of 1100 eV. In Fig. 7 the effect of the ion microfield on the Li-like $N=4$ to 2 lines is shown. The dashed line shows the combined Li-like and Be-like $N=4$ to 2 spectra, including ion microfield effects, and the solid line shows the spectrum resulting when the ion microfield is neglected in calculating the Li-like lines. It can be seen that the ion microfield

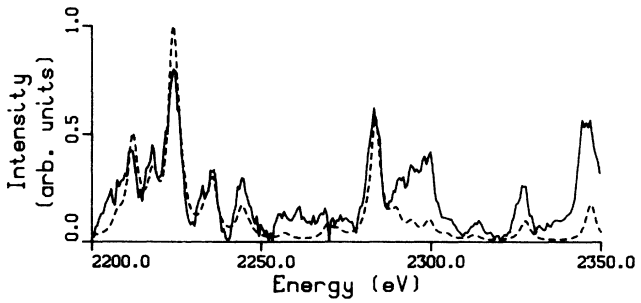

FIG. 3. Comparison of combined Li-like and Be-like Kr theoretical spectra; electron density, 1.5×10^{23} cm^{-3}; temperature, 1100 eV (dashed line), with LLE shot 11582 (solid line), 2200–2350 eV.

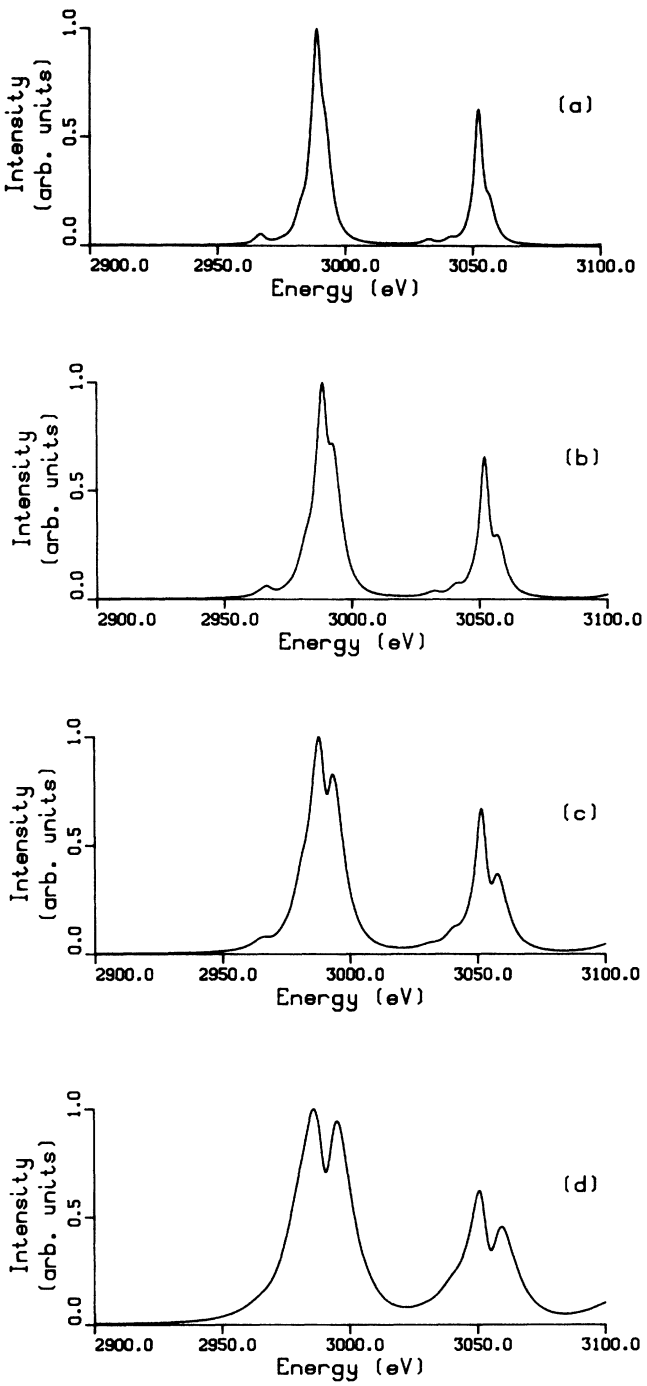

FIG. 4. Li-like Kr spectrum, 2900–3100 eV, $N=4$ to 2 transitions. Temperature, 1100 eV; electron density: (a) 10^{23}; (b) 2×10^{23}; (c) 4×10^{23}; (d) 10^{24} cm^{-3}.

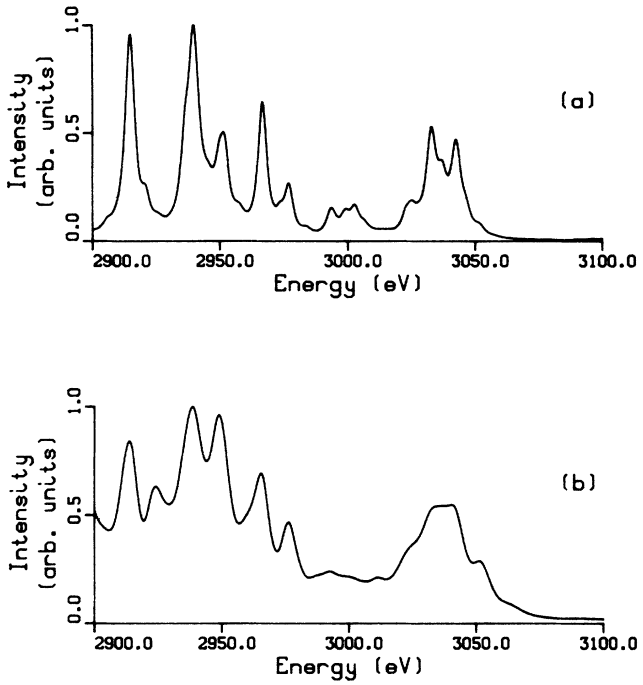

FIG. 5. Be-like Kr spectrum, 2900–3100 eV, $N=4$ to 2 transitions. Temperature, 1100 eV; electron density: (a) 1.5×10^{23}; (b) 10^{24} cm^{-3}.

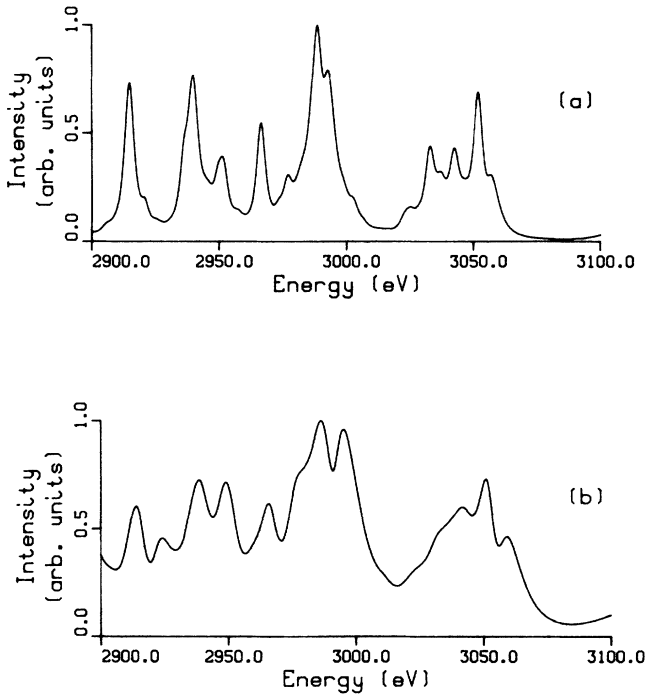

FIG. 6. Combined Li-like and Be-like Kr spectra, 2900–3100 eV, $N=4$ to 2 transitions. Temperature, 1100 eV; electron density: (a) 2×10^{23}; (b) 10^{24} cm^{-3}.

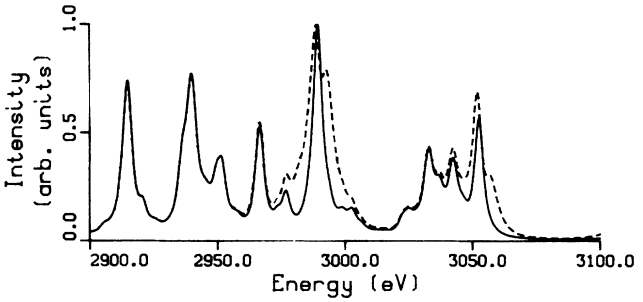

FIG. 7. Combined Li-like and Be-like Kr spectra, 2900–3100 eV, $N=4$ to 2 transitions. Temperature, 1100 eV, electron density, 2×10^{23} cm^{-3}. Dashed line, ion microfield included; solid line, ion microfield neglected in calculating Li-like spectrum.

is responsible for a large portion of the width of the Li-like lines, and that it contributes some additional structure. Figure 8 shows a comparison of the combined spectrum of Fig. 6(a) with the LLE spectrum from shot 11582 in the 2940–3060-eV energy range. The ratio of Li-like to Be-like Kr spectral intensities was adjusted to obtain the closest agreement with experiment. Theory and experiment show fairly good agreement in the general shape and position of spectral features. There is good agreement in the width of the Li-like feature at 2990 eV. The microfield-dependent Li-like peaks at 2993 and 3056 eV both appear to be present in this densitometer scan of the experimental spectrum. Their presence is not so clearly indicated in some other scans for this experiment, but the general widths and shapes of the spectral features are still in good agreement. Based on the agreement between theory and experiment in Fig. 8 and the demonstrated density dependence of the $N=4$ to 2 spectra, we estimate a density of approximately 2×10^{23} cm^{-3} for shot 11582. This is in good agreement with the density of 1.5×10^{23} cm^{-3} obtained in a study of the hydrogenic and He-like Ar lines from this shot.[10]

Let us consider the validity of the static ion approximation. For the Li-like Kr lines from $N=4$ to 2 transi-

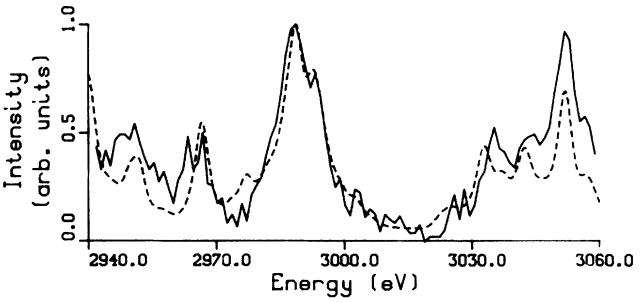

FIG. 8. Comparison of combined Li-like and Be-like Kr theoretical spectra; electron density, 2×10^{23} cm^{-3}; temperature, 1100 eV (dashed line), with LLE shot 11582 (solid line), 2940–3060 eV. (Note that the energy range is reduced from that in Figs. 4–7.)

tions in Figs. 7 and 8, the large ion broadening indicates that the lines are becoming hydrogenic (exhibiting a linear Stark effect). In that case, the criterion for validity of the static-ion approximation is that the characteristic time for the radiator state, $1/\Delta\omega$, be much less than the time scale for motion of the ion which produces the Stark shift $\Delta\omega$. The time scale for the ion motion is r_p/v_p, where r_p is the ion-radiator separation and v_p is the ion-radiator relative velocity. This can be written[12]

$$\Delta\omega = \frac{3\hbar Z_p(n_i q_i - n_f q_f)}{2Z_r m r_p^2} \gg \frac{v_p}{r_p} .$$

Here, Z_r is the nuclear charge of the radiator, Z_p is the charge of the perturbing ion, and $n_i q_i, n_f q_f$ are the principal and parabolic electric quantum numbers for the initial and final radiator states. Eliminating r_p gives

$$\Delta\omega \gg \frac{2mv_p^2 Z_r}{3\hbar Z_p(n_i q_i - n_f q_f)} .$$

Using $\mu v_p^2/2 = 3kT/2$, where μ is the ion-radiator reduced mass, this becomes[13,14]

$$\Delta\omega \gg \omega_s = \frac{2mkTZ_r}{\mu\hbar Z_p(n_i q_i - n_f q_f)} .$$

For the Li-like Kr lines in Figs. 7 and 8, ω_s ranges from 0.0024 eV ($q_i = 3$) to 0.0071 eV ($q_i = 1$). The shift of the final state due to the microfield was negligible so q_f was set equal to zero. Since the line half-widths were approximately 3–4 eV before convolution with the 1.5-eV Lorentzian, ion dynamic effects should be negligible for these spectral lines.

VII. CONCLUSION

We have described a theoretical formalism and computer code for the calculation of multielectron ion spectra and shown applications of the code to analysis of Li-like and Be-like Kr spectra obtained in laser implosion experiments. In its current form or with minor modifications, this code can be used in the analysis of spectra from various multielectron radiators in plasmas over a large range of densities and temperatures.

ACKNOWLEDGMENTS

The research discussed in this work is partially supported by the National Laser Users Facility at the University of Rochester Laboratory for Laser Energetics and by a contract from the Lawrence Livermore National Laboratory.

[1]John T. O'Brien and C. F. Hooper, Jr., J. Quant. Spectrosc. Radiat. Transfer **14**, 479 (1974); Richard J. Tighe and C. F. Hooper, Jr., Phys. Rev. A **14**, 1514 (1976).

[2]H. R. Griem, *Spectral Line Broadening by Plasma* (Academic, New York, 1974).

[3]Earl W. Smith, J. Cooper, and C. R. Vidal, Phys. Rev. **185**, 140 (1969).

[4]David B. Boercker, Carlos A. Iglesias, and James W. Dufty, Phys. Rev. A **36**, 2254 (1987).

[5]C. F. Hooper, Jr., Phys. Rev. **165**, 215 (1968); Richard J. Tighe and C. F. Hooper, Jr., Phys. Rev. A **15**, 1773 (1977).

[6]Hans R. Griem, Milan Blaha, and Paul C. Kepple, Phys. Rev. A **19**, 2421 (1979).

[7]Hoe Nguyen *et al.*, Phys. Rev. A **33**, 1279 (1986).

[8]Earl W. Smith and C. F. Hooper, Jr., Phys. Rev. **157**, 126 (1967).

[9]Robert D. Cowan, *The Theory of Atomic Structure and Spectra* (University of California Press, Berkeley, 1981).

[10]N. D. Delamater, C. F. Hooper, T. Garber, L. A. Woltz, R. L. Kauffman, J. Scofield, M. Richardson, and P. Jaanimagi (unpublished).

[11]James W. Dufty and David B. Boercker, J. Quant. Spectrosc. Radiat. Transfer **16**, 1065 (1976).

[12]Hans R. Griem, Astrophys, J. **148**, 547 (1967).

[13]C. R. Vidal, J. Cooper, and E. W. Smith, J. Quant. Spectrosc. Radiat. Transfer **10**, 1011 (1970).

[14]Dipak H. Oza, Ronald L. Greene, and Daniel E. Kelleher, Phys. Rev. A **38**, 2544 (1988).